

RESEARCH ARTICLE

Seminal fluid and sperm diluent affect sperm metabolism in an insect: Evidence from NAD(P)H and flavin adenine dinucleotide autofluorescence lifetime imaging

Christian Massino¹  | Cornelia Wetzker^{1,2} | Ondřej Balvin³ | Tomáš Bartonicka⁴ | Jana Kremenova⁴ | Markéta Sasinkova³ | Oliver Otti⁵ | Klaus Reinhardt¹

¹Applied Zoology, Institute of Zoology, Faculty of Biology, Technische Universität Dresden, Dresden, Germany

²Light Microscopy Facility, CMCB, Technische Universität Dresden, Dresden, Germany

³Department of Ecology, Faculty of Environmental Sciences, Czech University of Life Sciences Prague, Prague, Czech Republic

⁴Department of Botany and Zoology, Masaryk University, Brno, Czech Republic

⁵Animal Population Ecology, Animal Ecology I, University of Bayreuth, Bayreuth, Germany

Correspondence

Christian Massino, Applied Zoology, Institute of Zoology, Faculty of Biology, Technische Universität Dresden, Dresden, Germany.
Email: christian.massino@tu-dresden.de

Funding information

Deutsche Forschungsgemeinschaft, Grant/Award Numbers: KR 1666/4-1, OT 521/4-1; Grantová Agentura České Republiky, Grant/Award Number: 18-08468J

Review Editor: Alberto Diaspro

Abstract

Sperm metabolism is fundamental to sperm motility and male fertility. Its measurement is still in its infancy, and recommendations do not exist as to whether or how to standardize laboratory procedures. Here, using the sperm of an insect, the common bedbug, *Cimex lectularius*, we demonstrate that standardization of sperm metabolism is required with respect to the artificial sperm storage medium and a natural medium, the seminal fluid. We used fluorescence lifetime imaging microscopy (FLIM) in combination with time-correlated single-photon counting (TCSPC) to quantify sperm metabolism based on the fluorescent properties of autofluorescent coenzymes, NAD(P)H and flavin adenine dinucleotide. Autofluorescence lifetimes (decay times) differ for the free and protein-bound state of the co-enzymes, and their relative contributions to the lifetime signal serve to characterize the metabolic state of cells. We found that artificial storage medium and seminal fluid separately, and additively, affected sperm metabolism. In a medium containing sugars and amino acids (Grace's Insect medium), sperm showed increased glycolysis compared with a commonly used storage medium, phosphate-buffered saline (PBS). Adding seminal fluid to the sperm additionally increased oxidative phosphorylation, likely reflecting increased energy production of sperm during activation. Our study provides a protocol to measure sperm metabolism independently from motility, stresses that protocol standardizations for sperm measurements should be implemented and, for the first time, demonstrates that seminal fluid alters sperm metabolism. Equivalent protocol standardizations should be imposed on metabolic investigations of human sperm samples.

KEYWORDS

bedbug, *Cimex lectularius*, FLIM, FLIRR, metabolic mapping, multiphoton microscopy, spermatozoa

This is an open access article under the terms of the Creative Commons Attribution License, which permits use, distribution and reproduction in any medium, provided the original work is properly cited.

© 2021 The Authors. *Microscopy Research and Technique* published by Wiley Periodicals LLC.

1 | INTRODUCTION

Sperm metabolism is central to male reproduction. For species with motile sperm, sperm metabolism will fuel motility to achieve fertilization. As any other eukaryotic cells, sperm cells can produce ATP by two pathways, glycolysis and oxidative phosphorylation. However, to what extent both pathways are used switches occur between them is not known for most species nor are details of internal and external metabolic substrates in sperm. For example, even in the well-studied model organism *Drosophila*, aspects of the sperm metabolism have only been revealed in the last few years, except for two early contributions (Geer, Kelley, Pohlman, & Yemm, 1975; Osanai & Chen, 1993). Recent contributions show that sperm cells employ surprisingly strong glycolysis in both the male and the female storage organ (Wetzker & Reinhardt, 2019) but also employ oxidative phosphorylation (Turnell & Reinhardt, 2020; Wetzker & Reinhardt, 2019). Sperm metabolism is not currently included in parameters of standard clinical semen testing (World Health Organization, 2010). However, such inclusion seems desirable, because motility alone is not a sufficient readout for fertilization ability. For example, sperm that is not motile does not necessarily lack metabolism and can still be used for in-vitro fertilization. In addition, most currently used clinical sperm parameters have low, or no, predictive power for fertility or the ability of the partner to conceive (Ferlin, 2012; Glazener, Ford, & Hull, 2000).

Attempting to standardize the measurement of sperm metabolism, we start with two factors that appear most fundamental to sperm metabolism: the experimental sperm diluent used (henceforth, medium) and seminal fluid. The sperm diluent varies widely between studies and may explain differences between publications even in sperm viability (Eckel et al., 2017). The effect of seminal fluid on sperm function has been reviewed earlier (Davis, 1965; Mann & Lutwak-Mann, 1981; Poiani, 2006) and received particular attention because of its potent antioxidant effect (Aitken, Jones, & Robertson, 2012; Davis, 1965; Wathes, Abayasekara, & Aitken, 2007).

Few methods are currently available to study sperm metabolism. They include nuclear magnetic resonance - spectroscopy (reviewed by Kamp, Büssemann, & Lauterwein, 1996), biochemical measurements of oxygen consumption and acidification rate (Magdanz, Boryshpolets, Ridzewski, Eckel, & Reinhardt, 2019; Paynter et al., 2017), and metabolic flux analysis using radiolabeled substrates (Weiner, Crosier, & Keefer, 2019). Ribou and Reinhardt (2012) and Reinhardt and Ribou (2013) introduced a method based on the fluorescence decay of a probe sensitive to oxygen radicals. These authors revealed that sperm metabolic rate and oxygen radicals production decreased rapidly as soon as sperm entered the female sperm storage organ (Reinhardt & Ribou, 2013; Ribou & Reinhardt, 2012). In another insect species, the common bedbug *Cimex lectularius*, oxygen radicals produced by sperm also decreased in females but increased after sperm had resided several weeks in the female sperm store (Reinhardt & Ribou, 2013). Simultaneously with the increase of oxygen radicals, fertility declined (Reinhardt & Ribou, 2013).

Fluorescence lifetime imaging microscopy (FLIM) makes use of the autofluorescent properties of the cellular coenzyme nicotinamide

adenine dinucleotide in its reduced form (NADH) and of flavin adenine dinucleotide (FAD) in its oxidized form to characterize cellular metabolism. NADH/FAD FLIM is commonly employed to study cancer cells (Skala et al., 2007; Skala et al., 2007; Wallrabe et al., 2018) and stem cell differentiation (Meleshina et al., 2016; Meleshina et al., 2017; Stringari et al., 2011). Metabolic FLIM has recently been employed as a label-free technique to study sperm metabolism (Reinhardt, Breunig, Uchugonova, & König, 2015; Ribou & Reinhardt, 2012; Wetzker & Reinhardt, 2019). Based on time-correlated single-photon counting (TCSPC; Becker, 2012), FLIM quantifies the duration of excited states of fluorophores, here, NAD(P)H and FAD. NAD(P)H subsumes NADH and its phosphorylated form NADPH due to their highly similar fluorescence behavior (Huang, Heikal, & Webb, 2002). In FLIM, fluorophores are excited by a pulsed laser, and the arrival time of emitted photons that reaches the detector is measured relative to the corresponding laser pulse at high temporal sensitivity. The photon arrival times add up to fluorescence decay curves for each pixel of the image. They allow for the statistical calculation of the fluorescence lifetime if sufficient photons are detected. The technique can disentangle decay curves of several components, such as several molecules or different structural forms of one molecule, as well as the relative contribution of each component. In case of NAD(P)H and FAD, these are free and protein-bound states of both coenzymes. For NAD(P)H, the short and long lifetimes, τ_1 and τ_2 , represent the decay of free and protein-bound molecules, respectively. Their relative abundances are termed a_1 and a_2 (Becker, 2012; Lakowicz, Szmacinski, Nowaczyk, & Johnson, 1992; Leben, Köhler, Radbruch, Hauser, & Niesner, 2019; Sharick et al., 2018). FAD lifetimes are the shorter τ_1 for the protein-bound state and the longer τ_2 for the free state of the coenzyme (Becker, 2012), again with relative abundances of the two.

The lifetime patterns of both markers, particularly the abundance of both lifetime states, serve as a metabolic fingerprint of cells and tissues. While a higher free-to-bound ratio of NAD(P)H is indicative of a more glycolytic state, a lower free-to-bound ratio is a hallmark of more oxidative states (Evers et al., 2018; Stringari et al., 2011; Wallrabe et al., 2018). For NAD(P)H, the relative contributions to the intensity peak of free and bound NAD(P)H lifetimes characterize the relative rate between glycolysis and oxidative phosphorylation (Stringari, Nourse, Flanagan, & Gratton, 2012). This procedure is, for example, used to identify cancer metabolism by the Warburg effect (Warburg, 1956) compared with normal tissue (Skala, Ricking, Bird, et al., 2007; Skala, Ricking, Gendron-Fitzpatrick, et al., 2007; Wallrabe et al., 2018). The relative contribution of free and bound NAD(P)H also served to quantify stem cell differentiation (Meleshina et al., 2016; Quinn et al., 2013; Stringari et al., 2011; Stringari et al., 2012). For example, a_1 can differ 5–10% points between normal and pre-grade cancer cells (Skala, Ricking, Bird, et al., 2007; Skala, Ricking, Gendron-Fitzpatrick, et al., 2007) or between stem cells and differentiated cells (Meleshina et al., 2016; Meleshina et al., 2017), and as much as 20% points between different tissues in *Drosophila* (Wetzker & Reinhardt, 2019). The method detects FAD autofluorescence lifetime changes in a similar way (Becker, Bergmann,

Suarez Ibarrola, Müller, & Braun, 2019; Islam, Honma, Nakabayashi, Kinjo, & Ohta, 2013; Wallrabe et al., 2018). Both NAD(P)H and FAD can be recorded from the same sample by the use of excitation light of different wavelengths and separate emission filter sets. The pattern of FAD variation provides important additional information on the metabolic state of cells. For example, NAD(P)H a_1 did not differ between sperm extracted from *Drosophila melanogaster* males compared with sperm extracted from females; however, the respective FAD a_1 values differed by 25% points indicative of differences of FAD-related biochemistry (Wetzker & Reinhardt, 2019). The so-called FLIM redox ratio (FLIRR), a lifetime-based redox ratio independent of fluorescence intensities, implements lifetime parameters of both NAD(P)H and FAD (Wallrabe et al., 2018). For further information about metabolic measurements via FLIM, see Blacker and Duchon (2016); Kolenc and Quinn (2019); and Schaefer, Kalinina, Rueck, von Arnim, and von Einem (2019).

Here, we use FLIM and exemplify in an urban pest insect, the common bedbug *C. lectularius* (Doggett, Miller, & Lee, 2018; Reinhardt & Siva-Jothy, 2007), how the sperm energy metabolism varies with the medium used and in the presence or absence of seminal fluid. This species was chosen, because it is one of the few for which previous data exist on FLIM-based sperm metabolism, and where sperm metabolism was linked to fertility (Reinhardt et al., 2015; Reinhardt & Ribou, 2013). Bedbugs produce sperm in sufficiently large numbers (Kaldun & Otti, 2016; Reinhardt, Naylor, & Siva-Jothy, 2011) to satisfy the split-sample design that is necessary to examine seminal fluid effects in individual males. A final advantage is that in this species, sperm is stored in separate anatomical compartments from seminal fluid (Davis, 1965) and so does (a) not activate sperm metabolism before the investigation and (b) the manufactured seminal fluid is stored “ready-to-go” without extraction from the accessory glands, and in containers that are large enough for easy fluid extraction and precisely controllable addition to sperm. Our data show that the artificial medium and the natural seminal fluid separately and additively affect sperm metabolism.

2 | METHODS

2.1 | Experimental animals

Male bedbugs were taken from a large stock colony (>1,000 individuals) that has been maintained as a standard culture for several years in the authors' laboratory at the TU Dresden (Germany). Bedbugs were housed at 70% r.H. as described earlier (Reinhardt, Naylor, & Siva-Jothy, 2003) but at slightly lower temperatures, between 21 and 23°C. The population used, named F4, originates from a field collection in London (England) in 2006 and has been extensively used in previous experiments (Bellinvia, Johnston, Reinhardt, & Otti, 2020; Bellinvia, Spachtholz, Borgwardt, Schauer, & Otti, 2020; Otti, Deines, Hammerschmidt, & Reinhardt, 2017; Otti, McTighe, & Reinhardt, 2013; Reinhardt et al., 2011; Reinhardt, Naylor, & Siva-Jothy, 2009a, 2009b) including for a study investigating the protein

composition of the seminal fluid (Reinhardt, Wong, & Georgiou, 2009). The function of seminal fluid in *C. lectularius* was described by Davis, 1965.

Throughout this study, males were sexually isolated for several weeks before use. During isolation, males were fed twice to stimulate sperm production (Kaldun & Otti, 2016). Feedings were separated by 1 week. Measurements were started 10 days after the last feeding.

The bedbug male has an asymmetric copulatory organ (facing left) but testes, adjacent sperm storage organs, the seminal vesicles (SVs), and seminal fluid containers are paired, symmetrical structures (Figure 1). The SVs are large enough to split them in half to examine sperm in the presence and absence of seminal fluid.

Similar to many other insects, bedbug sperm is very long (800 μm ; Cragg, 1920) and has a filamentous structure that prevents an easy distinction between head and tail. Moreover, insect sperm has no mid-piece but two mitochondrial derivatives (the nebenkerns) that are wound around the tail. For an overview of insect sperm morphology and motility, see Werner and Simmons (2008).

2.2 | Experimental design

We used a paired, full-factorial design whereby sperm was kept in either of two buffers (see Sample preparation) and, for the same male, measured with and without seminal fluid (SF), i.e., SF⁺ and SF⁰, respectively. The split-sample nature of the paired SF⁺-SF⁰ design was achieved by adding SF to one-half of the sperm container but not the other half. This design represents a paired analysis of variance (ANOVA) design of sperm metabolism in response to medium and SF. Because the current study is a technical baseline study, we also

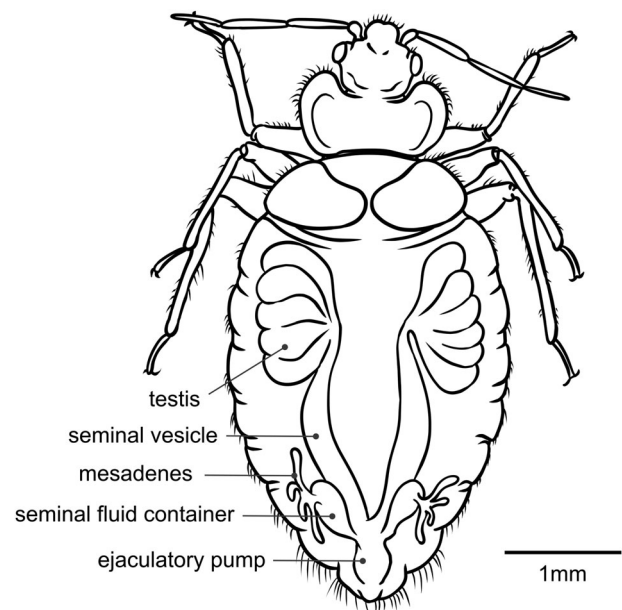


FIGURE 1 Schematic representation of the anatomy of the reproductive system of the male bedbug, *Cimex lectularius*, in dorsal view

examined the variation of sperm metabolism between the two paired SVs. We accounted for the fact that both SVs (first or second dissected) stem from the same male (see Section 2.7).

2.3 | Sample preparation

Dissection and sample preparations were performed in the respective medium of the allocated treatment, being either Grace's Insect medium (GM; Sigma-Aldrich, Pr.-Nr. G8142) or phosphate-buffered saline (PBS; Chemsolute Pr.-Nr. 8461). Both the two-paired SVs and the attached SF reservoirs (Figure 1) were dissected and transferred as a whole into a drop of medium onto a microscope slide. The SV that was picked first for the analysis was labeled SV1, and the second SV2. While SV1 was processed, SV2 remained intact in its assigned medium. SV1 and SV2 were random with respect to left or right. We took the first (SV1) measurements ~ 10 min after dissection, and the second (SV2) about 15–20 min thereafter.

The SV was cut in half, and each half was placed in a separate drop of 5 μ l medium. Sperm was squeezed out from one SV half into the drop of medium. That bedbug sperm can survive in similar volumes, without evaporation, and can stay even motile for 24 hr was shown by Rao & Davis (1969).

In SF^+ samples, the seminal fluid container was added to the sperm, ruptured and thereby SF released onto the sperm, immediately before the analysis. Both, SF^0 and SF^+ samples were then covered with a coverslip (18 \times 18 mm) and analyzed using FLIM. The order of SF^+ or SF^0 treatment was random within any SV. SV2 was analyzed in the same way as SV1. Dissection was successful in 14 males, 5 GM, and 9 PBS, but not all four paired measurements were obtained for all males (Table S1).

2.4 | NAD(P)H and FAD autofluorescence

We measured several metabolic parameters. The mean lifetime (τ_m), a commonly used parameter, is defined as:

$$\tau_m = a_1\tau_1 + a_2\tau_2 \text{ with } a_1 + a_2 = 1, \quad (1)$$

where τ_1 is the lifetime of free NAD(P)H or bound FAD and a_1 the relative contribution of τ_1 to τ_m , and τ_2 is the lifetime of bound NAD(P)H or free FAD with a_2 marking the relative contribution of τ_2 to τ_m . The FLIRR (Wallrabe et al., 2018) defined as:

$$\text{FLIRR} = \frac{a_2 \text{NAD(P)H}}{a_1 \text{FAD}}, \quad (2)$$

uses only the bound fractions of both fluorophores. This measure captures the redox state of the cell, because the oxidized FAD (in the denominator) and the reduced NAD(P)H are being used in the equation. With increasing oxidative phosphorylation activity, FLIRR, therefore, increases if (a) the bound NAD(P)H fraction

increases as free NAD(P)H is consumed, and/or (b) nonfluorescent $FADH_2$ is converted to fluorescent FAD, thereby increasing the relative abundance of free FAD and decreasing a_1 , the relative abundance of bound FAD. Both cell and tissue metabolism can be investigated in this way.

2.5 | Time-correlated single-photon count-fluorescence lifetime imaging microscopy

The measurements were executed using a multiphoton, pulsed titanium: sapphire femtosecond laser (Chameleon Ultra II, Coherent, Santa Clara, CA) and the microscopic setup described earlier (Wetzker & Reinhardt, 2019). In brief, the average laser power on the sample was around 12 mW. The microscope setup consisted of a AxioExaminer.Z1 (Carl Zeiss, Jena, Germany) with a motorized stage. For photon detection, two hybrid GaAsP photon detectors (HPM-100-40, Becker & Hickl GmbH, Berlin, Germany) were used. In addition to an optical magnification of 40 \times (water immersion objective), a 2 \times digital magnification was used with an image resolution of 256 \times 256 pixels. A total of 350 frames were measured amounting to a total scanning time of around 3 min per image. Two-photon excitation was achieved using light of 740 nm for NAD(P)H and 900 nm for FAD. For the recording of the NAD(P)H fluorescence signal, a bandpass filter of 450/30 nm was used, for FAD 525/39 nm. Emission light was split with a 505-nm beam splitter.

2.6 | FLIM data extraction and analysis

Autofluorescence lifetimes were calculated from the fluorescence decay curves using the software SCPIImage 8.0 (Becker & Hickl GmbH). The calculation of the lifetimes requires a correction of the temporal convolution of the decay signal generated by the measuring system. This correction is achieved by incorporating an instrument response function (IRF) generated using a urea crystal. A scatter of 0 and a fixed shift was set for each image. The offset was not fixed. The weighted least square methods implemented in SCPIImage 8.0 was used to fit the decay data. Increased photon numbers to calculate more reliable lifetime decays were achieved by pixel binning of two (i.e., 25 pixels per image) for NAD(P)H, and a binning of four (81 pixels) for FAD images. Lifetimes were calculated using a bi-exponential decay; that is, the fluorescence decay of each component was assumed to arise from two fluorophores (i.e., free and bound NAD(P)H, or FAD). This has the consequence that in our case, a_2 , the relative contribution of the long lifetime simply was $a_2 = 100\% - a_1$ and so is not presented separately in Section 3. The χ^2 values, which at perfect decay fits are 1.0, had a mean of 1.45 and a median of 1.18 across all images for NAD(P)H and a mean of 1.07 and a median of 1.06 for FAD.

Lifetime pictures were exported as matrixes from SCPIImage. The resulting, spatially explicit data files ("images") were imported into FIJI (Rueden et al., 2017; Schindelin et al., 2012) as text images. The

images were sorted into a multichannel stack with the slides representing the individual samples and the channels representing the lifetime parameters (τ_m , τ_1 , τ_2 , and a_1). The background was excluded using a threshold of 110 photons for NAD(P)H photon intensity images, thereby also excluding pixels with insufficient photon counts. Free active bedbug sperm aggregates (Ruknudin & Veera Raghavan, 1988), and the relatively high threshold was set to predominantly capture such regions of dense sperm. Sperm aggregations are the natural situation and would also retain sufficient sperm density over the time of the measurements, thus reducing background effects at low sperm density. All pixels in an image that passed the background threshold were defined as a region of interest (ROI). We used the threshold to generate a binary mask that was then used to create a selection of the pixels. This selection was stored for every slice of the stack as ROIs and used to extract the lifetime data. To have comparable data, the ROIs generated from NADH were also used for FAD. For ROI handling, the ROI Manager (Ferreira & Rasband, 2010–2012) in FIJI was used.

2.7 | Statistical analysis

Using R studio (Version 1. 3.1073) with R (4.0.3.) and packages *tidyverse* (package version 1.3.0; Wickham et al., 2019), *lme4* (1.1.1-25; Bates, Mächler, Bolker, & Walker, 2015), *lmerTest* (3.1-3; Kuznetsova, Brockhoff, & Christensen, 2017), *MASS* (7.3-53; Venables & Ripley, 2011), and *ggplot2* (3.3.2; Wickham, 2009), we employed generalized linear mixed effects modeling. We started by entering all explanatory variables, the so-called full model, which is appropriate for our a priori hypothesis that SF and the medium type affect sperm metabolism. All results of these models are presented. For SV and interaction effects between SF and medium, we did not have an a priori prediction, in which case stepwise, backward model reduction procedures are recommended (Symonds & Moussalli, 2011), and we present those in addition. Models were reduced by successively removing the higher-order interaction effects based on improvements of the Akaike Information Criterion (AIC). Any resulting model was compared with the previous, more complex model using the ANOVA command in R. If there was no significant difference in the model fit the less complex, reduced model was accepted. Model reductions were continued until the AIC did not improve, all terms remaining in the model showed significant p values, or the null model was reached. The normal distribution of the residuals was visually examined using QQ-plots. All model codes are provided in the Appendix.

2.8 | The effect of a possible time delay on the measurement of the sperm metabolism

During the analysis (see Section 3), the factor “SV” sometimes remained in the minimal model (e.g., for NAD τ_1 and NAD a_1), suggesting that first and second SV could differ in sperm metabolism.

Because a functional asymmetry for a paired, symmetric organ is relatively unlikely, we assumed the differences may have been related to the fact that SV2, although intact had stayed in the medium for longer before measurement than SV1. However, the time passed between measuring SV1 and SV2 was not correlated with the metabolic difference between SV1 and SV2 (Table S4), suggesting the time effect is small or masked by some other factor.

Future sperm metabolism protocols are unlikely to measure both SV but only one. We mimicked this situation by rerunning all statistical analyses using data from only the first SV (then excluding SV as a factor). We compared the two results throughout Section 3 but we note the latter approach has less statistical power, because the sample size is halved.

3 | RESULTS

Figure 2 shows color-coded NAD(P)H-FLIM pictures of bedbug sperm. These images were selected as those nearest to the mean of the respective lifetime value per treatment and so are representative. For a quantitative comparison, we below present an overview of the results from the model reduction analyses and their statistical significance. Individual data points are provided in (Figures S1–S6).

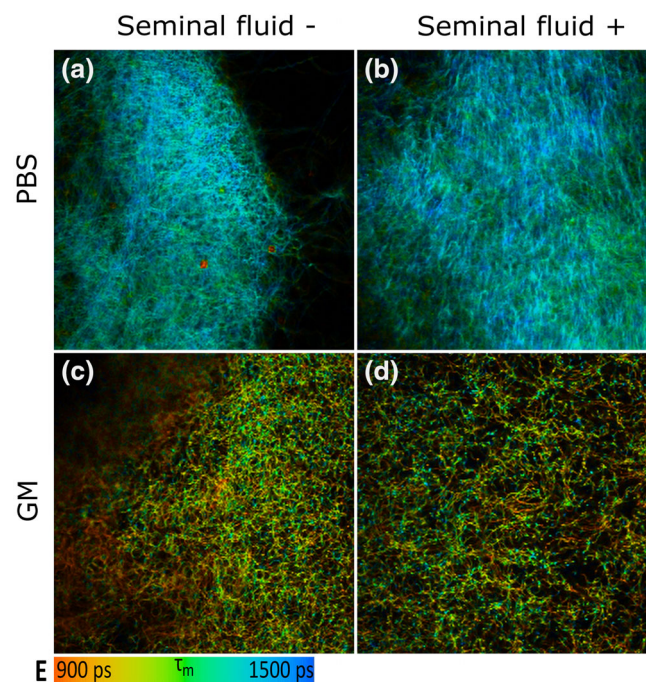


FIGURE 2 NAD(P)H fluorescence lifetime images of bedbug sperm (a–d), color coded by the mean fluorescence lifetime τ_m (e). Images are representative because they represent those closest to the treatment mean. Treatments were free sperm in phosphate-buffered saline (a,b) or Grace’s insect medium (c,d), either without (a,c) or with (b,d) seminal fluid

3.1 | NAD(P)H

3.1.1 | Proportion of free NAD(P)H (a_1)

NAD(P)H a_1 ranged from 64.3 to 76.5% (Table S2 and Figure 3d) and was significantly affected by the medium (Table 1 and Figure 3d), varying for GM between 70.6 and 76.5%, and for PBS between 64.3 and 73.4%. SV and SF showed no significant effect but their exclusion from the model worsened the AIC, suggesting they contribute to variation in a_1 . For example, mean a_1 values for SV1 in GM were 74.3% (SF⁰) and 72.7% (SF⁺), and for SV2 74.9 and 75.2%, respectively. In PBS, SV1 mean a_1 values were 69.8% (SF⁰) and 67.7% (SF⁺), for SV2 70 and 67.7%, respectively (see Figure 3d for the entire variation). In addition to the main effect's medium, SF and SV, the interaction of medium \times SV remained in the model (non-significant, Table 1) suggesting the medium affects sperm metabolism differently in both SV. Rerunning the analysis using only data from SV1 confirmed the impacts of medium and SF,

whereas their interaction term did not improve the model fit and was removed (Table 2).

3.1.2 | Lifetime of free NAD(P)H autofluorescence (τ_1)

NAD(P)H τ_1 ranged from 570.2 to 814.4 ps (Table S2 and Figure 3b) and was significantly affected by medium (Table 1). For SF⁰ sperm, τ_1 was higher in SV1 than in SV2 (695 vs. 675 ps) in PBS, but not in GM (645 vs. 644 ps). SF in the sample lead to a slight decrease in τ_1 in PBS (SV1: 687 ps; SV2: 660 ps) but a slight increase in GM (SV1: 652 ps; SV2: 689 ps) (Table S2). The minimal model retained most terms from the full model (Table 1), and this included the two-way interaction of Medium:SV and Medium:SF. This is suggesting that a complex mix of effects governs τ_1 . None of these terms except medium were significant. Using SV1 data only confirmed medium as a significant effect on τ_1 and rejected more complex interactions, such as medium \times SF (Table 2).

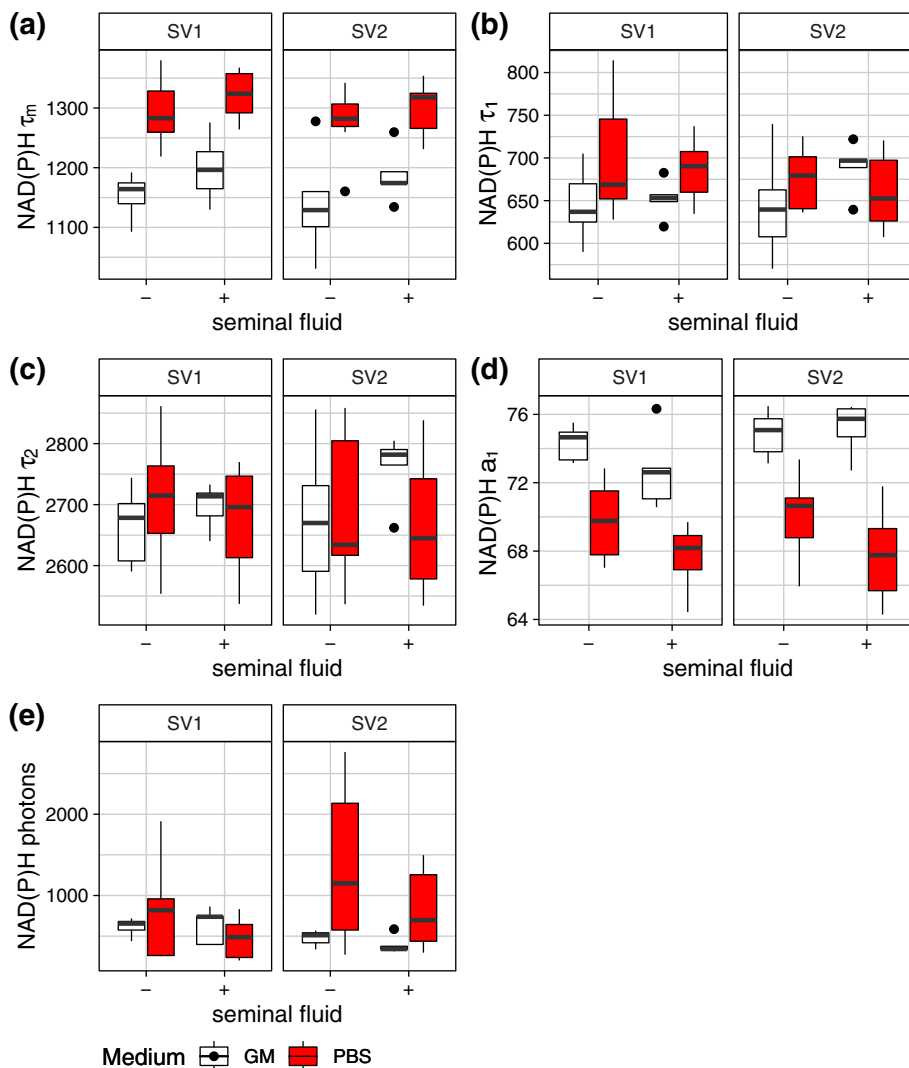


FIGURE 3 Mean fluorescence lifetimes τ_m (a), short lifetime τ_1 (b), long lifetimes τ_2 (c), the proportion of the short lifetimes of NAD(P)H a_1 (d), and photon intensity (e) of sperm of the bedbug, *Cimex lectularius*, in relation to the storage medium (no fill: Grace's Insect medium, red fill: phosphate-buffered saline), the first (SV1) and the second dissected sperm vesicle (SV2), as well as the absence (–) or presence (+) of seminal fluid. The data are medians, with boxes showing the 25 and 75 percentiles, and the error bars representing the 10 and 90 percentiles. Outliers are shown as dots

TABLE 1 Summary of the statistical analyses using a generalized linear modeling approach

Response variable	Medium	SV	SF	Medium:SV	Medium:SF
NAD(P)H					
τ_m	<.0001	-	.011	-	-
τ_1	.008	.381	.202	.113	.153
τ_2	.406	-	.134	-	.069
a_1	<.0001	.164	.411	.101	-
Photons	.391	.336	.853	.011	.114
FAD					
τ_m	<.0001	-	.437	-	.073
τ_1	.066	-	-	-	-
τ_2	.047	-	-	-	-
a_1	.042	-	.415	-	.039
Photons	.142	.159	.310	-	.094
FLIRR					
FLIRR	<.001	-	-	-	-

Notes: The p values of all explanatory variables and their interactions are shown, if they remained in the final (minimal) model. Values are shown for four response variables of both NAD(P)H and flavin adenine dinucleotide (FAD), as well as a composite measure, FLIRR. For NAD(P)H and FAD, τ_m represents the mean lifetime, τ_1 is the lifetime of the short, and τ_2 is the lifetime of the long component. a_1 shows the relative contribution of the short lifetime to the intensity maxima with $a_1 + a_2 = 1$. Columns show the explanatory variables medium, seminal vesicles (SV), seminal fluid (SF), and their interactions marked by “:”. Variables that did not remain in the model are shown by “-”; for all others, the p values are given, and significant ones are in bold. No three-way interaction and no SV:SF interaction remained in any minimal model.

TABLE 2 Summary of the statistical analyses using a generalized linear modeling approach when only the first seminal vesicle is included, thereby removing a possible dissection time effect

Response variable	Medium	SF	Medium:SF
NAD(P)H			
τ_m	<.0001	.058	-
τ_1	.026	-	-
τ_2	-	-	-
a_1	<.0001	.016	-
FAD			
τ_m	.003	.603	.033
τ_1	.073	-	-
τ_2	.058	-	-
a_1	.097	.717	.028
FLIRR			
FLIRR	.006	.260	.020

Notes: The p values of all explanatory variables and their interactions are shown if they remained in the final (minimal) model. Values are shown for four response variables of both NAD(P)H and flavin adenine dinucleotide (FAD), as well as a composite measure, FLIRR. For NAD(P)H and FAD, τ_m represents the mean lifetime, τ_1 is the lifetime of the short, and τ_2 is the lifetime of the long component. a_1 shows the relative contribution of the short lifetime to the intensity maxima with $a_1 + a_2 = 1$. Columns show the explanatory variables and its interactions marked by “:”. Variables that did not remain in the model are shown by “-”; for all others, the p values are given, and significant ones are in bold.

3.1.3 | Lifetime of protein-bound NAD(P)H autofluorescence (τ_2)

τ_2 ranged from 2,519.7 to 2,861.5 ps (Table S2). Medium treatments themselves contributed relatively little to a shift of τ_2 (Figure 3c)—no significant influences on τ_2 were detected (Table 1). The minimal model included medium, SF, and medium \times SF (Table 1 and Figure 3c). For SV2, SF⁺ samples differed substantially between GM and PBS (Figure 3c). Using only SV1 data showed no significant influence on τ_2 (Table 2).

3.1.4 | Mean lifetime of NAD(P) (τ_m)

For SF⁰ sperm, τ_m was about 10% lower in GM (mean 1,169.5 ps) than in PBS (mean 1,298.4 ps). τ_m increased for SF⁺ samples in both media (Figure 3a). The minimal model (Table 1) retained medium and SF as explanatory variables (SF significant). Using only SV1 data retained the same terms with SF being close to significance and medium remaining highly significant (Table 2).

3.2 | FAD

All lifetime values of FAD showed large variation, which was exaggerated by medium (Figure 4 and Table S3). For example, τ_m of FAD in

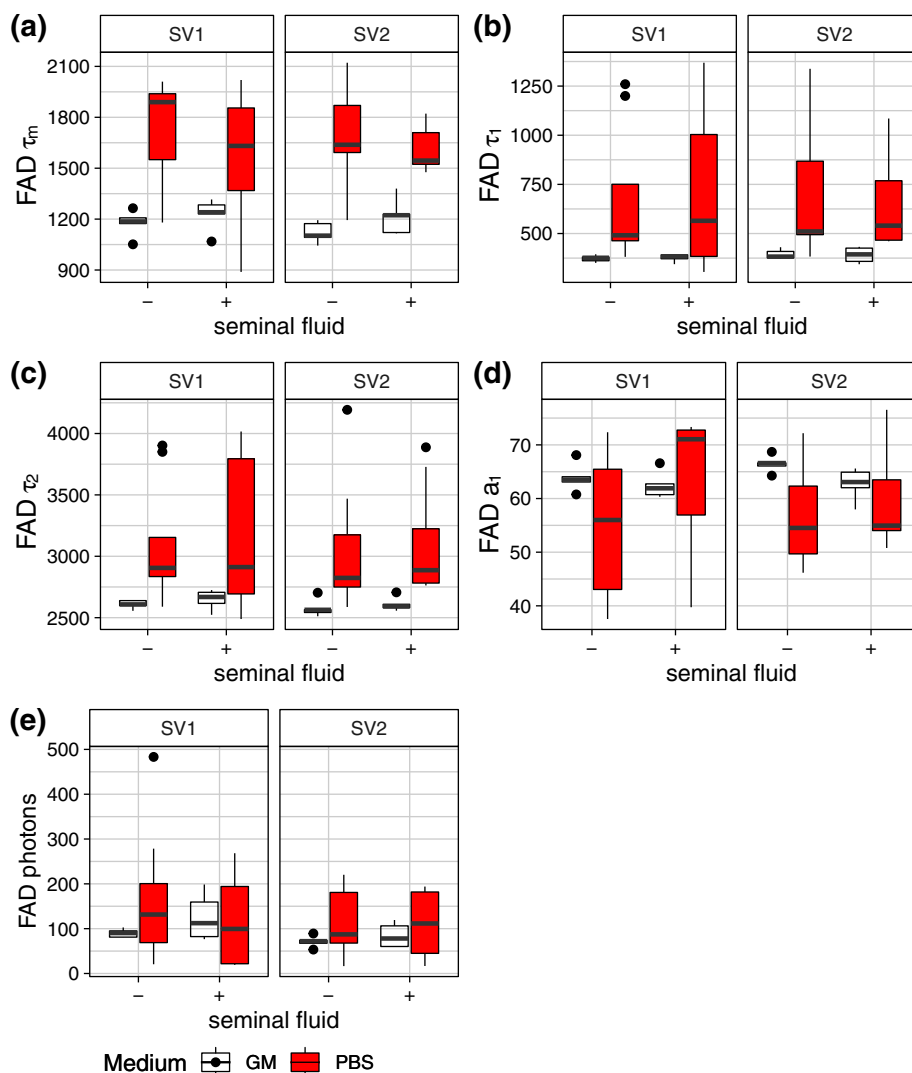


FIGURE 4 Mean fluorescence lifetimes τ_m (a), short lifetime τ_1 (b), long lifetimes τ_2 (c), the proportion of the short lifetimes of flavin adenine dinucleotide a_1 (d), and photon intensity (e) of sperm of the bedbug, *Cimex lectularius*, in relation to the storage medium (no fill: Grace's Insect medium, red fill: phosphate-buffered saline), the first (SV1) and the second dissected sperm vesicle (SV2), as well as the absence (-) or presence (+) of seminal fluid. The data are medians, with boxes showing the 25 and 75 percentiles, and the error bars representing the 10 and 90 percentiles. Outliers are shown as dots

GM varied between 1,044.1 and 1,379.7 ps but in PBS between 888.8 and 2,121.5 ps (Table S3).

3.2.1 | Proportion of protein-bound FAD (a_1)

FAD a_1 varied from 37.5 to 76.5% (Table S3), significantly explained by medium, and medium \times SF interaction (Table 1). SF itself was not significant but stayed in the minimal model (Table 1). a_1 was lower when SF was added to sperm in GM for both SV1 and SV2 (Figure 4d), but for sperm in PBS, a_1 was higher for SV1 when SF was added to sperm and was only slightly higher in SV2 (Figure 4d). Using SV1 data confirmed medium and SF to explain variation in a_1 (not significant) and their interaction (Table 2).

3.2.2 | Lifetime of free FAD (τ_2)

τ_2 ranged between 2,489.1 and 4,192.9 ps (Table S3), significantly affected by medium (Table 1). τ_2 showed 16% lower values in GM

than in PBS (Table S3 and Figure 4c). Rerunning the model with SV1 data only confirmed that only medium remained in the model (Table 2).

3.2.3 | Lifetime of protein-bound FAD (τ_1)

FAD τ_1 ranged from 304.7 to 1,368.8 ps (Table S3). It was affected only by medium (Table 1) and confirmed using only SV1 data (Table 2). Similar to τ_2 , τ_1 also showed lower values in GM than in PBS (Table S3 and Figure 4b). Here, the values in GM were \sim 4% lower than in PBS.

3.2.4 | Mean lifetime of FAD (τ_m)

τ_m varying between 888.7 and 2,121.5 ps was affected by medium, SF, and the interaction of medium and SF (Figure 4a and Table 1), confirmed for the case that only SV1 data were used (Table 2).

3.3 | FLIRR

Model reduction procedures suggested that FLIRR was significantly explained only by medium (Table 1 and Figure 5). Rerunning the model with SV1, the terms medium, SF, and medium \times SF are being significant (Table 2). We provide this analysis mainly for comparative purposes to other articles. It should be interpreted with caution because FLIRR is a ratio, its statistical treatment violating basic principles, because a ratio assumes a linear relationship between the proportions of the bound fractions of NAD(P)H and FAD.

3.4 | Photon intensity

The photon intensity of NAD(P)H was between 201 and 2,765 photons (Table S2 and Figure 3e) and for FAD between 16 and 483 (Table S3 and Figure 4e). In the minimal model for NAD(P)H, the interaction SF:SV and the three-way interaction were removed from the model. Of the remaining terms, only the interaction of Medium:SV was significant ($p = .011$, see Table 1). For FAD, all single terms and the two-way interaction of Medium:SF remained in the minimal model (Table 1). None of the remaining terms were significant. We used Spearman's rank correlation test to see if photon intensity correlated with estimates of lifetime values. NAD(P)H τ_2 correlated positively with photon intensity ($\rho = .322$, $p = .020$), FAD τ_1 ($\rho = -.347$, $p = .013$), and a_1 ($\rho = -.609$, $p = 3.4E-6$) negatively with the intensity (Table S5). These correlations could either mean that estimates are low when photon counts are low, that high metabolism increased photon counts, or that more photons are emitted by more dense sperm aggregates. When we ranked sperm density in the microscopy images from low (one) to high density (five) by a person blind to treatment and not involved in study, we found that NAD(P)H intensity was

higher at higher sperm density ($\rho = .299$, $p = .031$), suggesting a normal, biological effect. For FAD intensity where photon counts were low in a few cases, but here sperm density and photon intensity were not correlated ($\rho = .192$, $p = .178$), suggesting FAD parameters were not biased by low photon counts.

4 | DISCUSSION

We present a detailed FLIM protocol to examine sperm metabolism, using an insect as an example. We quantified two of the seemingly most important sources of variation, a methodological one, the sperm diluent used (GM or PBS), and a biological one, the presence and absence of seminal fluid. We found that the diluent affected all parameters examined, and SF most of them (Table 1), suggesting that procedures to measure sperm metabolism need to be highly standardized. Some parameters, such as τ_1 and τ_2 for NAD(P)H, and τ_m and a_1 for FAD, were also affected by an interaction between medium and SF, showing that the two media do not elicit identical metabolic processes in the presence of SF—another important insight when results are compared between laboratories. Those effects that turned out significant in our analysis were largely confirmed as significant by a simplified protocol examining only the first dissected SV (compare Tables 1 and 2), with two exceptions: (a) SF treatment became a significant predictor of NAD(P)H a_1 when using only SV1, suggesting either false positives due to low sample size or that the SF effect is not the same for both SV. (b) The interaction of medium \times SF became a significant predictor of FLIRR. Below, we discuss these issues and advocate the use of FLIM as a diagnostic tool for metabolic sperm health.

4.1 | Photon counts and the quality of metabolic estimates

The photon count per pixel in a sample determines the quality of parameter estimates—low photon counts can distort the lifetime estimates. NAD(P)H photon counts increase as glycolysis increases (NADH production) and/or as oxidative phosphorylation decreases (NADH consumption; Evers et al., 2018). We found that NAD(P)H photon intensity was significantly explained by the interaction of Medium and SV but that none of the lifetime values of NAD(P)H were significantly explained by this interaction. We conclude that photon intensity did not distort our NAD(P)H lifetime estimates. Also, τ_2 correlated positively with NAD(P)H photon counts. Although τ_2 was not affected by our treatments, it is possible that long lifetimes may require more photons for more precise lifetime calculation.

FAD photon count was not significantly influenced by treatment. However, it was higher for lower values of τ_1 ($p = .013$, $\rho = -.347$) and a_1 ($p = 3.5E-6$, $\rho = -.609$). Increased mitochondrial activity would increase FAD photon count as nonfluorescent FADH₂ is converted into fluorescent FAD. This would explain the strong correlation of FAD a_1 with photon count but not the correlation with τ_1 . It

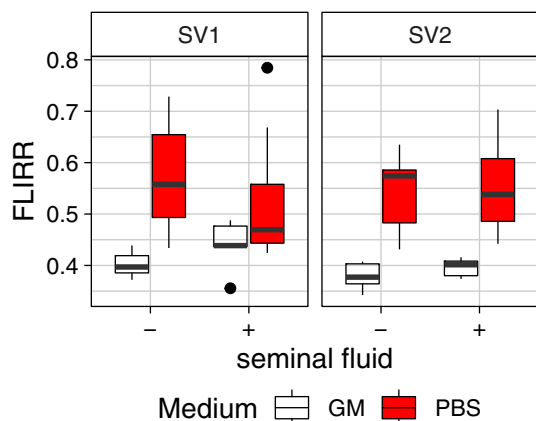


FIGURE 5 Fluorescence Lifetime Redox Ratio (FLIRR) of sperm of the bedbug, *Cimex lectularius*, in relation to the storage medium (no fill: Grace's Insect medium, red fill: phosphate-buffered saline), the first (SV1) and the second dissected sperm vesicle (SV2), as well as the absence (–) or presence (+) of seminal fluid. The data are medians, with boxes showing the 25 and 75 percentiles, and the error bars representing the 10 and 90 percentiles. Outliers are shown as dots

is unclear if the change in τ_1 could be attributed to changes in FAD-enzyme interaction, or if the short lifetime of unbound FAD had an impact on τ_1 , as FAD in aqueous solution comprises a multi-exponential decay with a fast and a longer lifetime (Islam et al., 2013; Islam, Susdorf, Penzkofer, & Hegemann, 2003), or both.

4.2 | The effect of seminal fluid on sperm metabolism

SF affects sperm function in several ways. For example, SF can either incapacitate or support rival sperm (Holman, 2009; Holman & Snook, 2008), an effect that seems to depend, in part, on the relatedness of rivals (Den Boer, Baer, & Boomsma, 2010). In *C. lectularius*, SF activates sperm travel through the female (Davis, 1965) but not in the related *Cimex hemipterus* (Ruknudin & Veera Raghavan, 1988). However, in the latter species, SF contained substrates that extended sperm motility in vitro (Ruknudin & Veera Raghavan, 1988). In *C. lectularius*, we found that SF increased τ_1 and lowered a_1 of NAD(P)H in PBS (Figure 2b,d), indicating that SF increased sperm oxidative phosphorylation, and provided substances that were not already contained in the medium. The stimulation of oxidative phosphorylation by SF likely explains the lower FAD a_1 values observed for GM (Figure 3d). With increased FADH consumption during oxidative phosphorylation, free FAD increases and, thus, reduces the relative amount of bound FAD (a_1). Bedbug SF contains proteins, sugars, and amino acids (Rao, 1974; Reinhardt, Wong, & Georgiou, 2009), as does hemolymph (Rao, 1974) through which the sperm travel. None of these components are found in PBS but GM contains sugars and amino acids, including L-alanine, for which in vitro evidence suggests it might be metabolized by bedbug sperm (Rao, 1974). However, it seems that amino acid catabolism may not be responsible for the increased oxidative phosphorylation in GM, because in GM, sperm was overall more glycolytic. Sperm may favor sugars over amino acids, or simply metabolize whatever is more abundant, which in GM would be sugar (e.g., Sucrose 26.68 g/L) not amino acids (0.05–0.7 g/L). In addition, the amount of sugar in SF in relation to that in GM seems negligible but future experiments will have to isolate the effects of individual components of GM.

NAD(P)H τ_2 was nearly significantly explained by the interaction of Medium:SF. τ_2 is affected by various enzymes involved in both glycolysis and oxidative phosphorylation which together produce a wide range of lifetimes (Leben et al., 2019; Sharick et al., 2018). The Medium:SF variation in τ_2 may have arisen from ROS production due to increased oxidative phosphorylation. In PBS, sperm experiences greater oxidative phosphorylation by PBS and SF, whereas in GM, only SF would increase ROS. Alternatively, the action of ROS may not have been direct but may have stimulated NADPH production, which may reduce ROS damage (Blacker & Duchon, 2016). Free NADPH τ_1 variation would not be caused by ROS, because free NADPH is indistinguishable spectrally and by lifetime from free NADH; by contrast, bound NADPH shows longer lifetimes than bound NADH (Blacker et al., 2014).

4.3 | The effect of time and medium

Bedbug sperm motility depends on oxygen (Rao & Davis, 1969; Ruknudin & Veera Raghavan, 1988) if oxidative phosphorylation fuels motility but glycolysis is possible in oxygen-poor environments. The relatively higher glycolytic state of bedbug sperm in GM than PBS suggests that GM fosters glycolysis and could support motility for a prolonged time. Similarly, in honeybees, where the female sperm storage organ is low in oxygen, sperm switch toward oxygen-independent glycolysis (Paynter et al., 2017). In our study species, the biology is even more complex, because both oxygen and sperm metabolism are likely to differ when sperm leave the female copulatory organ compared with when they travel through the female hemolymph or when entering the ovaries. It needs further investigation if the change from oxygen-dependent to oxygen-independent is a switch, or whether simply the oxygen-dependent pathway is turned off.

FAD τ_1 increases with oxidative phosphorylation (Wallrabe et al., 2018) and so would also lead to a decrease in FAD a_1 . This is what we found for sperm in GM (Figure 3d). The GM-FAD data for the sperm that were dissected later (SV2) also suggest some oxidative phosphorylation. However, for NAD(P)H, the SF-related increase in oxidative phosphorylation was less pronounced between SV1 and SV2 (Figure 3d). One possible explanation may be that in the 20–25 min between dissection and measurement, sperm in SV2 was shielded from substrates and oxygen and, therefore, may have metabolized substrates within the vesicle. As sperm metabolism is likely to favor sugars over amino acids, a slightly higher glycolytic state may be expected. Especially, if sperm have no other substrates available to feed the oxidative phosphorylation. Possibly, the SV effect we observed simultaneously produced a higher glycolytic rate in GM and a higher oxidative phosphorylation in PBS.

4.4 | Methodological results

The literature on metabolic FLIM often uses τ_m as an easy lifetime readout. For NAD(P)H, τ_m was almost identical to the inverse of a_1 (Figure 3a), suggesting that NAD(P)H τ_m differences are mainly caused by an increase in a_2 or a decrease in a_1 . a_1 is the common indicator for higher glycolytic or oxidative phosphorylation rate (Stringari, Nourse, et al., 2012). Thus, while a_1 strongly predicts τ_m , the reverse is not true. In other words, τ_m alone is not a suitable indicator of NAD(P)H. We recommend that researchers report τ_m measurements in concert with at least those of a_1 . We further recommend that researcher does not set τ_1 and τ_2 at fixed values, because τ_m is determined by the product of a_1 and τ_1 , and fixing τ_1 will not allow one to accommodate τ_m changes caused by additive effects of a_1 and τ_1 . That such concerns are not merely a theoretical issue, which is shown by our SF effects on NAD(P)H where a_1 and τ_1 were both non-significant but τ_m was significant. Had we fixed τ_1 we might not have detected the effect of SF on τ_m . Such fixing also has an impact when using the lifetime of free NAD(P)H to examine changes in the physical and chemical environment of the cell (Ogikubo et al., 2011; Scott, Spencer,

Leonard, & Weber, 1970). For example, viscosity varies between mitochondria and the cytoplasm (Evers et al., 2018). τ_1 is often measured as a mixture of cytoplasmic and mitochondrial τ_1 and can, therefore, change based on either the amount of free NAD(P)H in the cytoplasm and/or the mitochondria. During glycolysis, more free NAD(P)H is produced in the cytoplasm, shifting the overall sample mean toward smaller τ_1 .

4.5 | FLIM as a suitable tool to examine sperm quality

The relatively poor suitability of sperm motility as an indicator of fertility in humans may make sperm metabolism an additional indicator of fertility. We suggest our protocol is a promising basis from which to develop the measurement of sperm metabolism in other species, including humans. Our data indicate that GM produced minimal variation between the samples compared to the variation of the FAD lifetime values in PBS. Possibly, the low variation arose, because the excess of substrates in GM pushed sperm to optimal metabolism, whereas in PBS sperm show different states of starvation. Therefore, we suggest using GM or other glycolysis-supporting media for sample storage but an energetically more demanding medium if sperm function is to be elucidated ("stress test"). An important next step will be to examine the actual predictive power of sperm metabolism for fertility. Our method is non-destructive; should FLIM be applied in assisted reproduction techniques, the fertilization ability of sperm that have undergone FLIM needs to be established, and currently, it seems that glycolysis-supporting media provide the best starting point.

Sperm metabolism can differ even between related species, such as in *Drosophila* (Turnell & Reinhardt, under review), or between mouse (Tourmente, Villar-Moya, Rial, & Roldan, 2015) or bedbug species (Davis, 1964, 1965; Rao & Davis, 1969; Ruknudin & Veera Raghavan, 1988). These differences also include the relative contributions by glycolysis and oxidative phosphorylation to sperm metabolism (Du Plessis, Agarwal, Mohanty, & van der Linde, 2015; Storey, 2008; Tombes & Shapiro, 1989). We, therefore, realize that projections might sometimes be difficult from one species to the next. However, we suggest that our method may be applicable to livestock, for example, to monitor the quality of cryo-preserved sperm after thawing and before insemination as well as to optimize sperm storage media.

In our study, we focused on free sperm but it is important to note that FLIM allows the measurement of sperm metabolism in intact organs (Wetzker & Reinhardt, 2019). An ambitious, though probably distant, vision is to use FLIM to monitor sperm metabolic health in vivo in humans. If current FLIM approaches using simple skin contact to detect skin cancer (König, 2020) are employable, non-invasive monitoring of metabolic parameters of sperm in the testes and the epididymis may be possible in vivo; and perhaps even in the female oviduct. An existing proof-of-concept for an automated FLIM read-out pipeline (Wetzker & Reinhardt, 2019) may augment this vision.

5 | CONCLUSION

We confirmed that FLIM is a powerful tool to measure sperm metabolism. We also showed for free sperm, that is, for sperm in contact to oxygen, that medium and seminal fluid impact sperm metabolism in a way that easily mirrors differences that are, otherwise, seen between normal and cancer cells, or between stem cells and differentiated cells. Furthermore, we were able to show, using FLIM, that sperm metabolism is plastic and responds to the environment. This also implicates that this method could be used as a measurement of plasticity of sperm when, for example, sperm of different species would be compared. Also, the activation effect of SF appeared to be independent from the two media we used and pushed the metabolism toward a higher rate of oxidative phosphorylation, although this does not need to be the case for all media. Generally, our results call for highly standardized media and experimental conditions when analyzing sperm metabolism and other sperm functions.

ACKNOWLEDGMENTS

Thanks to Biz Turnell for help with statistics and Yvette von Bredow for help with Figure 1. The study was funded by the DFG to OO (OT 521/4-1) and KR (KR 1666/4-1), as well as by GACR to OB (18-08468J) and TB (18-08468J).

CONFLICT OF INTEREST

The author and co-authors declare no conflict of interest.

AUTHOR CONTRIBUTIONS

Christian Massino and Klaus Reinhardt, with assistance by Tomáš Bartonicka, Jana Kremenova, Ondřej Balvin, Markéta Sasinkova, and Oliver Otti, designed the study. Christian Massino carried out the measurements. Christian Massino, with the help of Cornelia Wetzker, Oliver Otti, and Klaus Reinhardt, analyzed the data. Christian Massino and Klaus Reinhardt wrote and Cornelia Wetzker, Tomáš Bartonicka, Jana Kremenova, Ondřej Balvin, Markéta Sasinkova, Oliver Otti, and Klaus Reinhardt revised the manuscript.

DATA AVAILABILITY STATEMENT

Data will be deposited online upon the acceptance of the paper. Data can be accessed via: <https://opara.zih.tu-dresden.de/xmlui/handle/123456789/1969>. <http://dx.doi.org/10.25532/OPARA-127>.

ORCID

Christian Massino  <https://orcid.org/0000-0002-7316-9507>

REFERENCES

- Aitken, R. J., Jones, K. T., & Robertson, S. A. (2012). Reactive oxygen species and sperm function—In sickness and in health. *Journal of Andrology*, 33(6), 1096–1106. <https://doi.org/10.2164/jandrol.112.016535>
- Bates, D., Mächler, M., Bolker, B., & Walker, S. (2015). Fitting linear mixed-effects models using lme4. *Journal of Statistical Software*, 67(1), 1–48. <https://doi.org/10.18637/jss.v067.i01>
- Becker, W. (2012). Fluorescence lifetime imaging - Techniques and applications. *Journal of Microscopy*, 247(2), 119–136. <https://doi.org/10.1111/j.1365-2818.2012.03618.x>

- Becker, W., Bergmann, A., Suarez Ibarrola, R., Müller, P.-F., & Braun, L. Z. (2019). Metabolic imaging by simultaneous FLIM of NAD(P)H and FAD. *Proceedings of SPIE*, 10882, 10. <https://doi.org/10.1117/12.2510132>
- Bellinvia, S., Johnston, P. R., Reinhardt, K., & Otti, O. (2020). Bacterial communities of the reproductive organs of virgin and mated common bedbugs, *Cimex lectularius*. *Ecological Entomology*, 45(1), 142–154. <https://doi.org/10.1111/een.12784>
- Bellinvia, S., Spachtholz, A., Borgwardt, I., Schauer, B., & Otti, O. (2020). Female immunity in response to sexually transmitted opportunistic bacteria in the common bedbug *Cimex lectularius*. *Journal of Insect Physiology*, 123, 104048. <https://doi.org/10.1016/j.jinsphys.2020.104048>
- Blacker, T. S., & Duchen, M. R. (2016). Investigating mitochondrial redox state using NADH and NADPH autofluorescence. *Free Radical Biology & Medicine*, 100, 53–65. <https://doi.org/10.1016/j.freeradbiomed.2016.08.010>
- Blacker, T. S., Mann, Z. F., Gale, J. E., Ziegler, M., Bain, A. J., Szabadkai, G., & Duchen, M. R. (2014). Separating NADH and NADPH fluorescence in live cells and tissues using FLIM. *Nature Communications*, 5, 3936. <https://doi.org/10.1038/ncomms4936>
- Cragg, F. W. (1920). Further observations on the reproductive system of *Cimex*, with special reference to the behaviour of the spermatozoa. *Indian Journal of Medical Research*, 8(1), 32–79.
- Davis, N. T. (1964). Studies of the reproductive physiology of *Cimicidae* (Hemiptera)-I. Fecundation and egg maturation. *Journal of Insect Physiology*, 10, 947–963.
- Davis, N. T. (1965). Studies of the reproductive physiology of *Cimicidae* (Hemiptera)-II. Artificial insemination and the function of the seminal fluid. *Journal of Insect Physiology*, 11, 355–366.
- Den Boer, S. P. A., Baer, B., & Boomsma, J. J. (2010). Seminal fluid mediates ejaculate competition in social insects. *Science*, 327(5972), 1506–1509. <https://doi.org/10.1126/science.1184709>
- Doggett, S. L., Miller, D. M., & Lee, C.-Y. (Eds.). (2018). *Advances in the biology and management of modern bed bugs*. Hoboken, NJ: Wiley-Blackwell.
- Du Plessis, S. S., Agarwal, A., Mohanty, G., & van der Linde, M. (2015). Oxidative phosphorylation versus glycolysis: What fuel do spermatozoa use? *Asian Journal of Andrology*, 17(2), 230–235. <https://doi.org/10.4103/1008-682X.135123>
- Eckel, B. A., Guo, R., & Reinhardt, K. (2017). More Pitfalls with Sperm Viability Staining and a Viability-Based Stress Test to Characterize Sperm Quality. *Frontiers in Ecology and Evolution*, 5, 599. <https://doi.org/10.3389/fevo.2017.00165>
- Evers, M., Salma, N., Osseiran, S., Casper, M., Birngruber, R., Evans, C. L., & Manstein, D. (2018). Enhanced quantification of metabolic activity for individual adipocytes by label-free FLIM. *Scientific Reports*, 8(1), 1–14. <https://doi.org/10.1038/s41598-018-27093-x>
- Ferlin, A. (2012). New genetic markers for male fertility. *Asian Journal of Andrology*, 14(6), 807–808. <https://doi.org/10.1038/aja.2012.84>
- Ferreira, T., & Rasband, W. S. (2010–2012). ImageJ User Guide – IJ 1.46.
- Geer, B. W., Kelley, K. R., Pohlman, T. H., & Yemm, S. J. (1975). A comparison of rat and *Drosophila* spermatozoan metabolisms. *Comparative Biochemistry and Physiology B*, 50(1), 41–50. [https://doi.org/10.1016/0305-0491\(75\)90296-5](https://doi.org/10.1016/0305-0491(75)90296-5)
- Glazener, C. M., Ford, W. C., & Hull, M. G. (2000). The prognostic power of the post-coital test for natural conception depends on duration of infertility. *Human Reproduction (Oxford, England)*, 15(9), 1953–1957. <https://doi.org/10.1093/humrep/15.9.1953>
- Holman, L. (2009). *Drosophila melanogaster* seminal fluid can protect the sperm of other males. *Functional Ecology*, 23(1), 180–186. <https://doi.org/10.1111/j.1365-2435.2008.01509.x>
- Holman, L., & Snook, R. R. (2008). A sterile sperm caste protects brother fertile sperm from female-mediated death in *Drosophila pseudoobscura*. *Current Biology*, 18(4), 292–296. <https://doi.org/10.1016/j.cub.2008.01.048>
- Islam, M. S., Honma, M., Nakabayashi, T., Kinjo, M., & Ohta, N. (2013). Ph dependence of the fluorescence lifetime of FAD in solution and in cells. *International Journal of Molecular Sciences*, 14(1), 1952–1963. <https://doi.org/10.3390/ijms14011952>
- Islam, S. D., Susdorf, T., Penzkofer, A., & Hegemann, P. (2003). Fluorescence quenching of flavin adenine dinucleotide in aqueous solution by pH dependent isomerisation and photo-induced electron transfer. *Chemical Physics*, 295(2), 137–149. <https://doi.org/10.1016/j.chemphys.2003.08.013>
- Kaldun, B., & Otti, O. (2016). Condition-dependent ejaculate production affects male mating behavior in the common bedbug *Cimex lectularius*. *Ecology and Evolution*, 6(8), 2548–2558. <https://doi.org/10.1002/ece3.2073>
- Kamp, G., Büsselmann, G., & Lauterwein, J. (1996). Spermatozoa: Models for studying regulatory aspects of energy metabolism. *Experientia*, 52(5), 487–494.
- Kolenc, O. I., & Quinn, K. P. (2019). Evaluating cell metabolism through autofluorescence imaging of NAD(P)H and FAD. *Antioxidants & Redox Signaling*, 30(6), 875–889. <https://doi.org/10.1089/ars.2017.7451>
- König, K. (2020). Review: Clinical in vivo multiphoton FLIM tomography. *Methods and Applications in Fluorescence*, 8(3), 34002. <https://doi.org/10.1088/2050-6120/ab8808>
- Kuznetsova, A., Brockhoff, P. B., & Christensen, R. H. B. (2017). lmerTest package: Tests in linear mixed effects models. *Journal of Statistical Software*, 82(13), 1–26. <https://doi.org/10.18637/jss.v082.i13>
- Lakowicz, J. R., Szmacinski, H., Nowaczyk, K., & Johnson, M. L. (1992). Fluorescence lifetime imaging of free and protein-bound NADH. *Proceedings of the National Academy of Sciences of the United States of America*, 89(4), 1271–1275. <https://doi.org/10.1073/pnas.89.4.1271>
- Leben, R., Köhler, M., Radbruch, H., Hauser, A. E., & Niesner, R. A. (2019). Systematic enzyme mapping of cellular metabolism by phasor-analyzed label-free NAD(P)H fluorescence lifetime imaging. *International Journal of Molecular Sciences*, 20(22), 5565. <https://doi.org/10.3390/ijms20225565>
- Magdanz, V., Boryshpolets, S., Ridzewski, C., Eckel, B., & Reinhardt, K. (2019). The motility-based swim-up technique separates bull sperm based on differences in metabolic rates and tail length. *PLoS One*, 14(10), e0223576. <https://doi.org/10.1371/journal.pone.0223576>
- Mann, T., & Lutwak-Mann, C. (1981). *Male reproductive function and semen: Themes and trends in physiology, biochemistry and investigative andrology*. London, England: Springer London.
- Meleshina, A. V., Dudenkova, V. V., Bystrova, A. S., Kuznetsova, D. S., Shirmanova, M. V., & Zagaynova, E. V. (2017). Two-photon FLIM of NAD(P)H and FAD in mesenchymal stem cells undergoing either osteogenic or chondrogenic differentiation. *Stem Cell Research & Therapy*, 8(1), 15. <https://doi.org/10.1186/s13287-017-0484-7>
- Meleshina, A. V., Dudenkova, V. V., Shirmanova, M. V., Shcheslavskiy, V. I., Becker, W., Bystrova, A. S., ... Zagaynova, E. V. (2016). Probing metabolic states of differentiating stem cells using two-photon FLIM. *Scientific Reports*, 6, 21853. <https://doi.org/10.1038/srep21853>
- Ogikubo, S., Nakabayashi, T., Adachi, T., Islam, M. S., Yoshizawa, T., Kinjo, M., & Ohta, N. (2011). Intracellular pH sensing using autofluorescence lifetime microscopy. *The Journal of Physical Chemistry B*, 115(34), 10385–10390. <https://doi.org/10.1021/jp2058904>
- Osana, M., & Chen, P. S. (1993). A comparative study on the arginine degradation cascade for sperm maturation of *Bombix mori* and *Drosophila melanogaster*. *Amino Acids*, 5(3), 341–350. <https://doi.org/10.1007/BF00806952>
- Otti, O., Deines, P., Hammerschmidt, K., & Reinhardt, K. (2017). Regular wounding in a natural system: Bacteria associated with reproductive organs of bedbugs and their quorum sensing abilities. *Frontiers in Immunology*, 8, 1855. <https://doi.org/10.3389/fimmu.2017.01855>

- Otti, O., McTighe, A. P., & Reinhardt, K. (2013). In vitro antimicrobial sperm protection by an ejaculate-like substance. *Functional Ecology*, 27(1), 219–226. <https://doi.org/10.1111/1365-2435.12025>
- Paynter, E., Millar, A. H., Welch, M., Baer-Imhoof, B., Cao, D., & Baer, B. (2017). Insights into the molecular basis of long-term storage and survival of sperm in the honeybee (*Apis mellifera*). *Scientific Reports*, 7, 40236. <https://doi.org/10.1038/srep40236>
- Poiani, A. (2006). Complexity of seminal fluid: A review. *Behavioral Ecology and Sociobiology*, 60(3), 289–310. <https://doi.org/10.1007/s00265-006-0178-0>
- Quinn, K. P., Sridharan, G. V., Hayden, R. S., Kaplan, D. L., Lee, K., & Georgakoudi, I. (2013). Quantitative metabolic imaging using endogenous fluorescence to detect stem cell differentiation. *Scientific Reports*, 3, 3432. <https://doi.org/10.1038/srep03432>
- Rao, H. V. (1974). Free amino acids in seminal fluid & haemolymph of *Cimex lectularius* L. & their possible role in sperm metabolism. *Indian Journal of Experimental Biology*, 12(4), 346–348.
- Rao, H. V., & Davis, N. T. (1969). Sperm activation and migration in bed bugs. *Journal of Insect Physiology*, 15(10), 1815–1832. [https://doi.org/10.1016/0022-1910\(69\)90014-6](https://doi.org/10.1016/0022-1910(69)90014-6)
- Reinhardt, K., Wong, C. H., & Georgiou, A. S. (2009). Detection of seminal fluid proteins in the bed bug, *Cimex lectularius*, using two-dimensional gel electrophoresis and mass spectrometry. *Parasitology*, 136(3), 283–292. <https://doi.org/10.1017/S0031182008005362>
- Reinhardt, K., Breunig, H. G., Uchugonova, A., & König, K. (2015). Sperm metabolism is altered during storage by female insects: Evidence from two-photon autofluorescence lifetime measurements in bedbugs. *Journal of the Royal Society Interface*, 12(110), 609. <https://doi.org/10.1098/rsif.2015.0609>
- Reinhardt, K., Naylor, R., & Siva-Jothy, M. T. (2003). Reducing a cost of traumatic insemination: Female bedbugs evolve a unique organ. *Proceedings of the Royal Society B*, 270(1531), 2371–2375. <https://doi.org/10.1098/rspb.2003.2515>
- Reinhardt, K., Naylor, R. A., & Siva-Jothy, M. T. (2009a). Ejaculate components delay reproductive senescence while elevating female reproductive rate in an insect. *Proceedings of the National Academy of Sciences of the United States of America*, 106(51), 21743–21747. <https://doi.org/10.1073/pnas.0905347106>
- Reinhardt, K., Naylor, R. A., & Siva-Jothy, M. T. (2009b). Situation exploitation: Higher male mating success when female resistance is reduced by feeding. *Evolution*, 63(1), 29–39. <https://doi.org/10.1111/j.1558-5646.2008.00502.x>
- Reinhardt, K., Naylor, R., & Siva-Jothy, M. T. (2011). Male mating rate is constrained by seminal fluid availability in bedbugs, *Cimex lectularius*. *PLoS One*, 6(7), e22082. <https://doi.org/10.1371/journal.pone.0022082>
- Reinhardt, K., & Ribou, A.-C. (2013). Females become infertile as the stored sperm's oxygen radicals increase. *Scientific Reports*, 3(1), 115. <https://doi.org/10.1038/srep02888>
- Reinhardt, K., & Siva-Jothy, M. T. (2007). Biology of the bed bugs (*Cimicidae*). *Annual Review of Entomology*, 52, 351–374. <https://doi.org/10.1146/annurev.ento.52.040306.133913>
- Ribou, A.-C., & Reinhardt, K. (2012). Reduced metabolic rate and oxygen radicals production in stored insect sperm. *Proceedings*, 279(1736), 2196–2203. <https://doi.org/10.1098/rspb.2011.2422>
- Rueden, C. T., Schindelin, J., Hiner, M. C., DeZonia, B. E., Walter, A. E., Arena, E. T., & Eliceiri, K. W. (2017). ImageJ2: ImageJ for the next generation of scientific image data. *BMC Bioinformatics*, 18(1), 529. <https://doi.org/10.1186/s12859-017-1934-z>
- Ruknudin, A., & Veera Raghavan, V. (1988). Initiation, maintenance and energy metabolism of sperm motility in the bed bug, *Cimex hemipterus*. *Journal of Insect Physiology*, 34(2), 137–142. [https://doi.org/10.1016/0022-1910\(88\)90166-7](https://doi.org/10.1016/0022-1910(88)90166-7)
- Schaefer, P. M., Kalinina, S., Rueck, A., von Arnim, C. A. F., & von Einem, B. (2019). NADH autofluorescence—A marker on its way to boost bioenergetic research. *Cytometry Part A*, 95(1), 34–46. <https://doi.org/10.1002/cyto.a.23597>
- Schindelin, J., Arganda-Carreras, I., Frise, E., Kaynig, V., Longair, M., Pietzsch, T., ... Cardona, A. (2012). Fiji: An open-source platform for biological-image analysis. *Nature Methods*, 9(7), 676–682. <https://doi.org/10.1038/nmeth.2019>
- Scott, T. G., Spencer, R. D., Leonard, N. J., & Weber, G. (1970). Synthetic spectroscopic models related to coenzymes and base pairs. V. Emission properties of NADH. Studies of fluorescence lifetimes and quantum efficiencies of NADH, AcPyADH, [reduced acetylpyridineadenine dinucleotide] and simplified synthetic models. *Journal of the American Chemical Society*, 92(3), 687–695. <https://doi.org/10.1021/ja00706a043>
- Huang, S., Heikal, A. A., & Webb, W. W. (2002). Two-photon fluorescence spectroscopy and microscopy of NAD(P)H and flavoprotein. *Biophysical Journal*, 82, 2811–2825.
- Sharick, J. T., Favreau, P. F., Gillette, A. A., Sdao, S. M., Merrins, M. J., & Skala, M. C. (2018). Protein-bound NAD(P)H lifetime is sensitive to multiple fates of glucose carbon. *Scientific Reports*, 8(1), 5456. <https://doi.org/10.1038/s41598-018-23691-x>
- Skala, M. C., Ricking, K. M., Bird, D. K., Gendron-Fitzpatrick, A., Eickhoff, J., Eliceiri, K. W., ... Ramanujam, N. (2007). In vivo multiphoton fluorescence lifetime imaging of protein-bound and free nicotinamide adenine dinucleotide in normal and precancerous epithelia. *Journal of Biomedical Optics*, 12(2), 24014. <https://doi.org/10.1117/1.2717503>
- Skala, M. C., Ricking, K. M., Gendron-Fitzpatrick, A., Eickhoff, J., Eliceiri, K. W., White, J. G., & Ramanujam, N. (2007). In vivo multiphoton microscopy of NADH and FAD redox states, fluorescence lifetimes, and cellular morphology in precancerous epithelia. *Proceedings of the National Academy of Sciences of the United States of America*, 104(49), 19494–19499. <https://doi.org/10.1073/pnas.0708425104>
- Storey, B. T. (2008). Mammalian sperm metabolism: Oxygen and sugar, friend and foe. *The International Journal of Developmental Biology*, 52(5–6), 427–437. <https://doi.org/10.1387/ijdb.072522bs>
- Stringari, C., Cinquin, A., Cinquin, O., Digman, M. A., Donovan, P. J., & Gratton, E. (2011). Phasor approach to fluorescence lifetime microscopy distinguishes different metabolic states of germ cells in a live tissue. *Proceedings of the National Academy of Sciences of the United States of America*, 108(33), 13582–13587. <https://doi.org/10.1073/pnas.1108161108>
- Stringari, C., Edwards, R. A., Pate, K. T., Waterman, M. L., Donovan, P. J., & Gratton, E. (2012). Metabolic trajectory of cellular differentiation in small intestine by phasor fluorescence lifetime microscopy of NADH. *Scientific Reports*, 2, 568. <https://doi.org/10.1038/srep00568>
- Stringari, C., Nourse, J. L., Flanagan, L. A., & Gratton, E. (2012). Phasor fluorescence lifetime microscopy of free and protein-bound NADH reveals neural stem cell differentiation potential. *PLoS One*, 7(11), e48014. <https://doi.org/10.1371/journal.pone.0048014>
- Symonds, M. R. E., & Moussalli, A. (2011). A brief guide to model selection, multimodel inference and model averaging in behavioural ecology using Akaike's information criterion. *Behavioral Ecology and Sociobiology*, 65(1), 13–21. <https://doi.org/10.1007/s00265-010-1037-6>
- Tombes, R. M., & Shapiro, B. M. (1989). Energy transport and cell polarity: Relationship of phosphagen kinase activity to sperm function. *The Journal of Experimental Zoology*, 251(1), 82–90. <https://doi.org/10.1002/jez.1402510110>
- Tourmente, M., Villar-Moya, P., Rial, E., & Roldan, E. R. S. (2015). Differences in ATP generation via glycolysis and oxidative phosphorylation and relationships with sperm motility in mouse species. *The Journal of Biological Chemistry*, 290(33), 20613–20626. <https://doi.org/10.1074/jbc.M115.664813>
- Turnell, B. R., & Reinhardt, K. (2020). Metabolic rate and oxygen radical levels increase but radical generation rate decreases with male age in

- Drosophila melanogaster* sperm. *The Journals of Gerontology*, 75(12), 2278–2285. <https://doi.org/10.1093/gerona/glaa078>
- Venables, W. N., & Ripley, B. D. (2011). *Modern applied statistics with S* (4th ed.). Statistics and computing. London, England: Springer.
- Wallrabe, H., Svindrych, Z., Alam, S. R., Siller, K. H., Wang, T., Kashatus, D., ... Periasamy, A. (2018). Segmented cell analyses to measure redox states of autofluorescent NAD(P)H, FAD & Trp in cancer cells by FLIM. *Scientific Reports*, 8(1), 79. <https://doi.org/10.1038/s41598-017-18634-x>
- Warburg, O. (1956). On the origin of cancer cells. *Science (New York, N.Y.)*, 123(3191), 309–314.
- Wathes, D. C., Abayasekara, D. R. E., & Aitken, R. J. (2007). Polyunsaturated fatty acids in male and female reproduction. *Biology of Reproduction*, 77(2), 190–201. <https://doi.org/10.1095/biolreprod.107.060558>
- Weiner, H. S., Crosier, A. E., & Keefer, C. L. (2019). Analysis of metabolic flux in felid spermatozoa using metabolomics and ¹³C-based fluxomics. *Biology of Reproduction*, 100(5), 1261–1274. <https://doi.org/10.1093/biolre/iox010>
- Werner, M., & Simmons, L. W. (2008). Insect sperm motility. *Biological Reviews of the Cambridge Philosophical Society*, 83(2), 191–208. <https://doi.org/10.1111/j.1469-185X.2008.00039.x>
- Wetzker, C., & Reinhardt, K. (2019). Distinct metabolic profiles in *Drosophila* sperm and somatic tissues revealed by two-photon NAD(P)H and FAD autofluorescence lifetime imaging. *Scientific Reports*, 9(1), 1–10. <https://doi.org/10.1038/s41598-019-56067-w>
- Wickham, H. (2009). *Ggplot2: Elegant graphics for data analysis. Use R*. New York: Springer New York. <https://doi.org/10.1007/978-0-387-98141-3>
- Wickham, H., Averick, M., Bryan, J., Chang, W., McGowan, L., François, R., ... Yutani, H. (2019). Welcome to the Tidyverse. *Journal of Open Source Software*, 4(43), 1686. <https://doi.org/10.21105/joss.01686>
- World Health Organization. (2010). *WHO laboratory manual for the examination and processing of human semen* (5th ed.). Nonserial Publications). Geneva, Switzerland: World Health Organization.

SUPPORTING INFORMATION

Additional supporting information may be found in the online version of the article at the publisher's website.

How to cite this article: Massino, C., Wetzker, C., Balvin, O., Bartonicka, T., Kremenova, J., Sasinkova, M., Otti, O., & Reinhardt, K. (2021). Seminal fluid and sperm diluent affect sperm metabolism in an insect: Evidence from NAD(P)H and flavin adenine dinucleotide autofluorescence lifetime imaging. *Microscopy Research and Technique*, 1–14. <https://doi.org/10.1002/jemt.23914>